Cell Tissue Bank (2019) 20:351–365
https://doi.org/10.1007/s10561-019-09774-7

Extracellular matrix derived by human umbilical cord-deposited mesenchymal stem cells accelerates chondrocyte proliferation and differentiation potential in vitro

Weixiang Zhang · Jianhua Yang · Yun Zhu · Xun Sun · Weimin Guo · Xuejian Liu · Xiaoguang Jing · Ganggang Guo · Quanyi Guo · Jiang Peng · Xiaofeng Zhu

Received: 17 January 2019 / Accepted: 10 May 2019 / Published online: 19 June 2019

Abstract The extracellular matrix (ECM) is a dynamic and intricate three-dimensional (3D) microenvironment with excellent biophysical, biomechanical, and biochemical properties that may directly or indirectly regulate cell behavior, including proliferation, adhesion, migration, and differentiation. Compared with tissue-derived ECM, cell-derived ECM potentially has more advantages, including less potential for pathogen transfer, fewer inflammatory or anti-host immune responses, and a closer resemblance to the native ECM microenvironment. Different types of cell-derived ECM, such as adipose stem cells, synovium-derived stem cells and bone marrow stromal cells, their effects on articular chondrocytes which have been researched. In this study, we aimed to develop a 3D cell culture substrate using decellularized ECM derived from human umbilical cord-derived mesenchymal stem cells (hUCMSCs), and evaluated the effects on articular chondrocytes. We evaluated the morphology and components of hUCMSC-derived ECM using physical and chemical methods. Morphological, histological, immunohistochemical, biochemical, and real-time PCR analyses demonstrated that proliferation and differentiation capacity of

Weixiang Zhang and Jianhua Yang have contributed equally to this work.

W. Zhang
The People's Hospital of Lanxi, 1359th Shanxi Road, Lanxi 321100, China

J. Yang · X. Liu · X. Jing · G. Guo · X. Zhu (✉)
School of Medicine, Jiamusi University, 148th Xuefu Road, Xiangyang District, Jiamusi 154007, China
e-mail: zhuxiaofeng1227@163.com

W. Zhang · X. Sun · W. Guo · X. Liu · X. Jing · G. Guo · Q. Guo · J. Peng
Institute of Orthopedics, Chinese PLA General Hospital, 28th Fuxing Road, Beijing 100853, China

Y. Zhu
School of Biomedical Sciences, The University of Hong Kong, 21 Sassoon Road, Pokfulam 999777, Hong Kong

X. Sun
School of Medicine, Nankai University, 94th Weijin Road, Nankai District, Tianjin 300071, China

X. Zhu
Medical Research Center of Mudanjiang Medical School, 3th Tongxiang Road, Aimin District, Mudanjiang 157011, China

X. Zhu
Institute of Neurosciences, Jiamusi University, 148th Xuefu Road, Xiangyang District, Jiamusi 154007, China

X. Liu
Zhengzhou Yihe Hospital Affiliated to Henan University, 69th Nongyedong Road, Zhengzhou 450000, China

chondrocytes using the 3D hUCMSC-derived ECM culture substrate was superior to that using non-coated two-dimensional plastic culture plates. In conclusion, 3D decellularized ECM derived from hUCMSCs offers a tissue-specific microenvironment for in vitro culture of chondrocytes, which not only markedly promoted chondrocyte proliferation but also preserved the differentiation capacity of chondrocytes. Therefore, our findings suggest that a 3D cell-derived ECM microenvironment represents a promising prospect for autologous chondrocyte-based cartilage tissue engineering and regeneration. The hUCMSC-derived ECM as a biomaterial is used for the preparation of scaffold or hybrid scaffold products which need to further study in the future.

Keywords Cell-derived ECM · Chondrocytes · Stem cells · 3D microenvironment · Proliferation

Introduction

Articular cartilage is a 1–3-mm thick, white layer of special tissue with a certain elasticity and hardness, located on the ends of long bones in joints including the knee, hip, elbow, and shoulder. To ensure normal motion of the joint, articular cartilage absorbs pressure and distributes mechanical load to protect the subchondral bone[1]. Articular cartilage has a very limited ability to self-repair owing to a lack of blood vessels and nerves in cartilage, and its nutrient supply is derived mainly from the synovial fluid (Buckwalter and Mankin 1998; Hunziker 1999). However, an articular cartilage defect is a common orthopedic disease, usually caused by strain, trauma, and articular degenerative diseases. If an early articular cartilage defect is not treated in a timely fashion, it leads to the development of joint degeneration and osteoarthritis (Gelber et al. 2000; Schinhan et al. 2012; Stufkens et al. 2010). Therefore, various therapeutic strategies, such as nonsurgical methods including hyaluronic acid intra-articular injection (Arrich et al. 2005) and surgical methods including microfracture, drilling, arthroscopic abrasion, and tissue engineering technology, have been applied to repair cartilage defects, but most treatments relieve articular pain only temporarily and do not achieve satisfactory results for patients (Simon and Jackson 2006).

Autologous chondrocyte transplantation (ACT) has long been regarded as a promising approach to replace conventional therapies for articular cartilage repair. Although the technology has been updated through four generations, several hurdles limiting the development and extensive application of ACT remain. Generally, ACT requires numerous chondrocytes (2×10^7), but adult chondrocytes are terminally differentiated cells with a very weak proliferative capacity in vitro, especially in patients suffering from cartilage disease and in elderly patients. This means these chondrocytes must undergo prolonged culturing to obtain sufficient cell numbers (Li and Pei 2012). Additionally, chondrocytes readily undergo replicative senescence and dedifferentiation during ex vivo expansion, and the expression of cartilage matrix-specific collagen II decreases sharply, together with increased expression of collagens I and III, resulting in a loss of chondrocytic characteristics (Benya and Shaffer 1982; von der Mark et al. 1977). Thus, identifying a novel cell culture substrate that improves the quantity and quality of chondrocytes has become a key factor in the development and application of ACT.

The extracellular matrix (ECM) is typically made up of both inorganic and organic compounds, such as hyaluronic acid (HA), collagens, proteoglycans (PGs), and glycosaminoglycans (GAGs), which compose an intricate and dynamic three-dimensional (3D) network with a certain arrangement. The variety of ECM components confers excellent physical, biochemical, and biomechanical properties that regulate the proliferation, survival, migration, self-renewal, and differentiation of cells by either direct or indirect pathways (Hynes 2009; Lane et al. 2014; Ozbek et al. 2010; Watt and Huck 2013). In turn, different types of cells also influence the compounds and structures of ECM in tissues and organs.

As a novel potential 3D cell culture substrate, decellularized ECM derived from different kinds of cells (also called cell-derived ECM) has been studied in the fields of cartilage (Antebi et al. 2015; He et al. 2009; Liao et al. 2010), bone (Kim et al. 2015; Pham et al. 2008; Zeitouni et al. 2012), nerve (Gu et al. 2014; Jian et al. 2015), skeletal muscle (Hurd et al. 2015), intervertebral discs (Yuan et al. 2013), and cardiovascular (Du et al. 2014) tissue engineering. Previously, Pei et al. reported that ECM produced by synovium-derived stem cells (SDSCs) not only greatly promoted the expansion but also inhibited the dedifferentiation

capacity of chondrocytes and SDSCs, both in vitro (Pei and He 2012) and in vivo (Pei et al. 2013). Chen et al. discovered that a bone marrow mesenchymal stem cell-derived ECM culture microenvironment facilitated the formation of mesenchymal colony-forming units and retained their multipotency during culture (Chen et al. 2007; Lai et al. 2010). Compared with adult mesenchymal stem cell (MSC)-derived ECM, fetal MSC-derived ECM exhibited an enormous capacity to promote ex vivo proliferation (Ng et al. 2014) and rejuvenation of the chondrogenic potential (Li et al. 2014) of adult MSCs. Unique proteins in fetal MSC-derived ECM may be related to enhanced adult MSC expansion and rejuvenation.

In this study, we chose human umbilical cord (hUC) MSC-derived ECM as a 3D cell culture system, because the UC contains primitive cells with properties that are similar to those of fetal MSCs, and UCMSC-derived ECM is acquired more easily than is chondrocyte-derived ECM. Here, we respectively isolated chondrocytes from rabbit knee articular cartilage and MSCs from hUC Wharton's jelly and then generated decellularized ECM derived from UCMSCs. Chondrocytes were cultured on UCMSC-derived ECM-coated culture plates (3D) or on plastic culture plates [two-dimensional (2D)], and the proliferation and differentiation capacity of these cells were compared.

Materials and Methods

Experimental design

Using a series of processes including physical and chemical methods, UCMSCs were isolated and extracted from hUCs. The obtained hUCMSCs were cultured on plates pre-coated with fibronectin, and when the plated hUCMSCs attained 80–90% confluence, a certain amount of ascorbic acid phosphate was used to accelerate ECM deposition. Subsequent treatment with detergents and alkaline reagents (ammonium hydroxide), which may remove cellular components from thin tissues, induced decellularization to prepare hUCMSC-derived ECM. Rabbit chondrocytes were seeded and expanded on two substrates, hUCMSC-derived ECM and plastic culture plates. Histological, immunohistochemical, biochemical, and real-time polymerase chain reaction (RT-PCR) analyses were conducted at different time points. An overview of the study design is shown in Fig. 1.

Preparation and identification of hUCMSCs

Isolation and culture of hUCMSCs

This study was performed with the approval of the Institutional Committee of the Chinese PLA General Hospital, China. These hUC samples were acquired from healthy volunteers at the Chinese PLA General Hospital, and the samples were handled within 12 h. The isolation and culture of hUCMSCs were performed similarly to previously described methods (Peng et al. 2011). Briefly, after rinsing three times with phosphate-buffered saline (PBS; Sigma-Aldrich, St. Louis, MO, USA) to remove blood clots, samples were cut into 2–3-cm pieces. The Wharton's jelly was removed and sliced into small pieces (0.5–1.0 cm^3) after removing the amnion and umbilical vessels, and the slices were subsequently seeded on plastic culture plates as well as cultured in minimum essential medium-α (Gibco, Grand Island, NY, USA) containing 100 U/mL penicillin/streptomycin (Sigma-Aldrich) and 10% fetal bovine serum (FBS; Gibco) at 37 °C under 5% CO_2 in an incubator. The UC slices were discarded once the UCMSC population reached 80–90% subconfluence after culturing for 14 days. For each passage, 0.25% trypsin–ethylenediamine tetraacetic acid (EDTA; Corning, Glendale, AZ, USA) was used to detach the cells.

Flow cytometry analysis

To assess the purity of human MSCs, minimal criteria have been proposed by the Mesenchymal and Tissue Stem Cell Committee of the International Society for Cellular Therapy, including (1) MSCs must adhere to plastic when incubated under normal culture conditions; (2) MSCs must express high levels ($\geq$ 95% positive) of CD90, CD73, and CD105 and lack expression ($\leq$ 2% positive) of CD45, CD34, CD14 or CD11b, CD79a or CD19, and HLA-DR surface molecules; (3) MSCs must have the potential to differentiate into adipocytes, osteoblasts, and chondroblasts under specific differentiation conditions in vitro (Dominici et al. 2006).

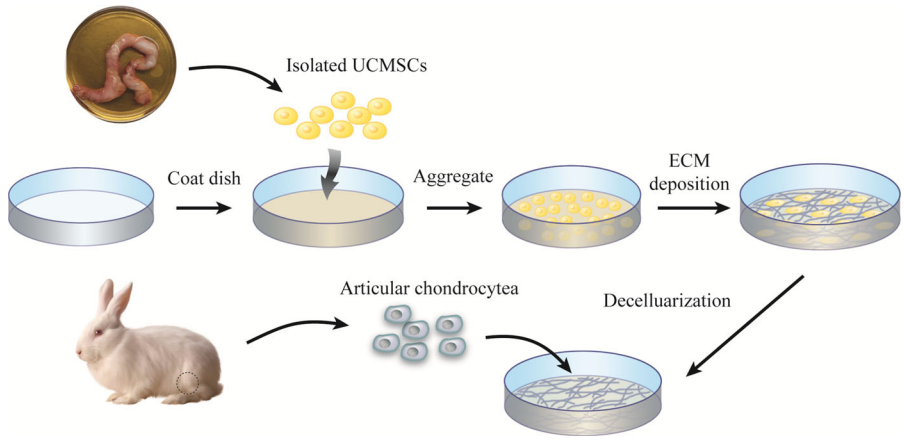

Fig. 1 Schematic illustration of the overall study design

For flow cytometry, the cells were detached using trypsin–EDTA and washed three times with PBS. Subsequently, the harvested cells were suspended, quantified, and adjusted to a concentration of 1×10^7/mL. The prepared cell suspension (0.1 mL, 1×10^6 cells per sample) was separately incubated with anti-CD90-FITC, anti-CD105-PerCP, anti-CD73-APC, and PE human MSC Negative Cocktail including anti-CD34-PE, anti-CD11b-PE, anti-CD19-PE, anti-CD45-PE, and HLA-DR-PE (1:1000; BD Biosciences, San Diego, CA, USA) in the dark for 30 min. The fluorescence of the cells was analyzed using a flow cytometer (FACS Calibur; BD Biosciences).

Analysis of the multipotent differentiation of hUCMSCs

The multipotent differentiation potential of hUCMSCs was confirmed as described previously[33]. Briefly, passage 2 (P2) hUCMSCs were treated with different induction media. For chondrogenic induction, cells were cultured in chondrogenic differentiation basic medium supplemented with 0.01% dexamethasone, 0.3% ascorbate, 1% ITS + supplement, 0.1% sodium pyruvate, 0.1% proline, and 1% TGF-β3 for 21 days. After fixation with 4% paraformaldehyde and embedding in paraffin, tissue sections were stained with Alcian blue for 30 min. For osteogenic induction, cells were cultured in 10% FBS-containing osteogenic differentiation basal medium supplemented with 1% penicillin–streptomycin, 1% glutamine, 0.2% ascorbate, 0.01% dexamethasone, and 1% β-glycerophosphate. After 21 days of differentiation, cells were fixed and stained with Alizarin red. Adipogenic differentiation medium consisted of induction medium A (10% FBS-containing basal medium A supplemented with 1% penicillin–streptomycin, 1% glutamine, 0.2% insulin, 0.1% IBMX, 0.1% rosiglitazone, and 0.1% dexamethasone) and medium B (10% FBS-containing basal medium B supplemented with 1% penicillin–streptomycin, 1% glutamine, and 0.2% insulin). For adipogenic differentiation, cells were cultured in induction medium A for 3 days, and then the medium was changed to induction medium B for 24 h. After four cycles of induction, cells were fixed, rinsed, and stained with Oil Red O.

Preparation and characterization of hUCMSC-derived ECM

Decellularized ECM derived from hUCMSC formation

P2 hUCMSCs (6×10^3/cm^2) were seeded on 6-well plates, which were pre-coated with fibronectin (25 μg/mL, Sigma-Aldrich) for 1 h at 37 °C. After culturing for 7 days, ascorbic acid (50 mM; Sigma-Aldrich) was added to complete medium for an additional 8 days, during which the cells attained approximately 80–90% confluency. During the entire procedure, the medium was changed completely every 2–3 days. For decellularization, samples were treated with 0.5% (v/v) Triton X-100 (Sigma-Aldrich) containing 20 mM NH_4OH (Sigma-Aldrich) in PBS for 5 min at 37 °C. After rinsing twice with PBS, the hUCMSC-derived ECM was stored in PBS containing 100 U/mL penicillin/streptomycin (Sigma-Aldrich) at 4 °C (Chen et al. 2007; He et al. 2009).

Morphological observation of hUCMSC-derived ECM

After fixation in 10% neutral buffered formalin, the morphology of specimens was observed under a phase-contrast microscope. For scanning electron microscopy (SEM), representative specimens were washed twice with PBS and fixed in 2.5% glutaraldehyde for 30 min, then incubated in 2% osmium tetroxide for another 30 min as the secondary fixation at room temperature. The specimens were dehydrated twice in progressive concentrations of ethanol (25%, 50%, 75%, 90%, and 100%) for 10 min each. After dehydration, ethanol was replaced with tertiary butanol (from 50 to 100%). In a follow-up analysis, specimens were freeze-dried using a vacuum drier, and sputtered with gold. The images were examined using the Zeiss MERLIN SEM (Carl Zeiss AG, Oberkochen, Germany).

Immunofluorescence staining analysis

Decellularized ECM was fixed in 10% neutral buffered formalin for 30 min at room temperature and then immunostained for collagen I, collagen II, laminin, fibronectin, decorin, perlecan, and biglecan to identify the components of decellularized ECM. The ECM was incubated with primary antibodies against collagen I (1:500; Abcam, Cambridge, UK), collagen II (1:100; Abcam), laminin (1:200; Abcam), fibronectin (1:200; Abcam), decorin (1:100; Abcam), perlecan (1:100; Abcam) and biglecan (1:100; Abcam) at 4° overnight, followed by incubation with secondary antibodies for 1 h and with Hoechst 33258 (Molecular Probes, Eugene, OR, USA) for 5 min for nuclear counterstaining. Images were taken using fluorescence microscopy (Olympus Imaging Systems, Tokyo, Japan).

In vitro studies of cell expansion on two different substrates

Isolation and expansion of rabbit articular chondrocytes

Three-month-old rabbits were obtained from a local slaughterhouse, and articular cartilage was harvested from knee joints using a knife in a sterile environment. To obtain chondrocytes, the cartilage samples were minced into pieces and enzymatically digested in 0.2% collagenase for 2 h on a magnetic stirrer. After centrifugation and suspension, the chondrocytes were plated in culture medium including Dulbecco's modified Eagle's medium (DMEM; Corning) supplemented with 10% FBS, 100 U/mL penicillin, and 100 mg/mL streptomycin. In a follow-up study, freshly isolated (P0) chondrocytes were seeded on two different substrates: plastic culture plates (plastic plates) and culture plates coated with hUCMSC-derived ECM (ECM plates) at a density of 3×10^3/cm^2 for six passages. For each passage, chondrocytes were cultured for 7 days (reaching approximately 90% confluence). To identify whether the different substrates affected the proliferation capacity of chondrocytes, a hemocytometer was used to count the total number of chondrocytes after cells were detached using trypsin–EDTA.

Cell cycle assay

Cell cycle assays were performed using propidium iodide staining. Chondrocytes cultured on ECM or plastic plates were trypsinized, washed, and resuspended at 1×10^6 cells/mL in PBS, followed by fixation with 70% chilled ethanol for 2 h at − 20 °C. The fixed cells were centrifuged, resuspended, and incubated with propidium iodide staining buffer at 4 °C for 1 h in the dark. The total numbers of cells at the different cell cycle phases were detected by flow cytometry (FACS Calibur; BD Biosciences). Flow cytometric experiments were performed in triplicate.

5-Ethynyl-2′-deoxyuridine (EdU)/Hoechst 33342 double staining

Using the EdU Labeling/Detection Kit (Ribo-bio, Guangzhou, China) following the manufacturer's instructions, logarithmic-phase cells were seeded on 6-well plates in medium containing EdU for 2 days at 37 °C under 5% CO_2. Afterwards, cultured cells were fixed in 10% neutral buffered formalin for 30 min and incubated in glycine for 5 min. After rinsing with PBS, cells were stained with Apollo reaction cocktail at room temperature for 30 min. Cells were then rinsed with 0.5% TritonX-100 in PBS and incubated with Hoechst 33342 (5 μg/mL) at room temperature for 30 min, followed by observation under a fluorescence microscope (Olympus Imaging Systems). Image Pro

Plus 5.0 software (Media Cybernetics, Silver Spring, MD, USA) was used to calculate the percentage of EdU-positive cells in five random fields of three samples.

Histological and immunohistochemical evaluation

The chondrocytes cultured on the ECM or plastic plates were fixed in 4% paraformaldehyde for 15 min at room temperature, washed twice with PBS, and stained with toluidine blue to detect sulfated GAG content. For immunohistochemical analysis, cells were treated with 0.5% (v/v) hydrogen peroxide for 10 min and then further immunolabeled with polyclonal antibodies against collagen I and II (Abcam) overnight at 4 °C after washing in PBS. The next day, cells were washed again with PBS and incubated with a phycoerythrin-conjugated goat anti-mouse IgG secondary antibody (Invitrogen) for 60 min at room temperature. Cells were then incubated with Vectastain ABC reagent (Vector Laboratories, Burlingame, CA, USA) using diaminobenzidine as a substrate and then counterstained with hematoxylin.

Biochemical analysis of DNA and GAG contents

For biochemical analysis, DNA was extracted using the Genomic DNA kit (TIANamp, Beijing, China) from cells cultured on the two different types of substrates and quantitated using the PicoGreen DNA assay kit (Invitrogen). To measure the sulfated GAG content, dimethylmethylene blue (DMMB) dye and the Tissue GAG Total Content DMMB Colorimetry kit were used according to the manufacturer's instructions (Genmed Scientific Inc., Shanghai, China).

RT-PCR

After the chondrocytes were expanded on two different substrates, ECM and plastic, for 7 and 14 days, total RNA was extracted from the cells using Trizol reagent (Invitrogen), and the RNA was reverse transcribed into cDNA using the ReverTra Ace qPCR RT Kit (Toyobo, Osaka, Japan) according to the manufacturer's protocol. Reactions were performed at 95 °C for 5 min, followed by 95 °C for 15 s, 58 °C for 15 s, and 72 °C for 45 s for 40 cycles. The $2^{-\Delta\Delta Ct}$ method was used to analyze the RT-PCR results. The primer sequences used for RT-PCR were as follows: SOX9 (forward: 5′-GCGGAGGAAGTCGGTGAAG AAT-3′, reverse: 5′ AAGATGGCGTTGGGCGA-GAT-3′), Aggrecan (forward: 5′-GGAGGAGCAG-GAGTTTGTCAA-3′, reverse: 5′-TGTCCATCCG A CCAGCGAAA-3′), Collagen I (forward: 5′-GCCA CCTGCCAGTCTTTACA-3′, reverse: 5′-CCATCA TCACCATCTCTGCCT-3′), Collagen II (forward: 5′-CACGCTCAAGTCCCTCAACA-3′, reverse: 5′-T CTATCCAGTAGTCACCGC TCT-3′), Collagen X (forward: 5′-CCACCAGGACAAGCAGTCAT-3′, reverse: 5′-CACTAACAAGAGGCATCCCG), and GAPDH (forward: 5′-CAAGAAGGTGGTGA AG CAGG-3′, reverse: 5′-CACTGTTGAAGTCGCAG-GAG-3′). Aggrecan, Sox9, and Collagens I and II are chondrogenic marker genes and Collagen X a hypertrophic marker gene; GAPDH was used as a reference gene.

Statistical analysis

All data were expressed as mean ± standard deviation. The two-sample *t* test was used to determine significant differences between two groups. Statistical analyses were performed using SPSS 17.0 software (SPSS, Inc., Chicago, IL, USA), and $p < 0.05$ indicated statistical significance.

Results

Characterization of hUCMSCs

To identify the purity of hUCMSCs, their characteristics were analyzed. Under a phase-contrast microscope, P3 hUCMSCs exhibited typical spindle-shaped fibroblastic morphology and plastic-adherent properties when incubated on plastic culture plates (Fig. 2a). To detect the pluripotent differentiation potential of hUCMSCs, cells were induced using three different types of lineage-specific media for adipocytes, chondroblasts, and osteoblasts in vitro. As shown in Fig. 2b–d, we observed strong staining with Oil Red O, Alizarin red, and Alcian blue, respectively. Flow cytometry analysis (Fig. 2e) revealed that hUCMSCs express high levels of CD73 (99.94%), CD90 (99.90%), and CD105 (71.09%) and lack expression of Negative PE (0.46%) for a Negative Cocktail including CD45, CD34, CD11b, CD19, and HLA-DR surface molecules.

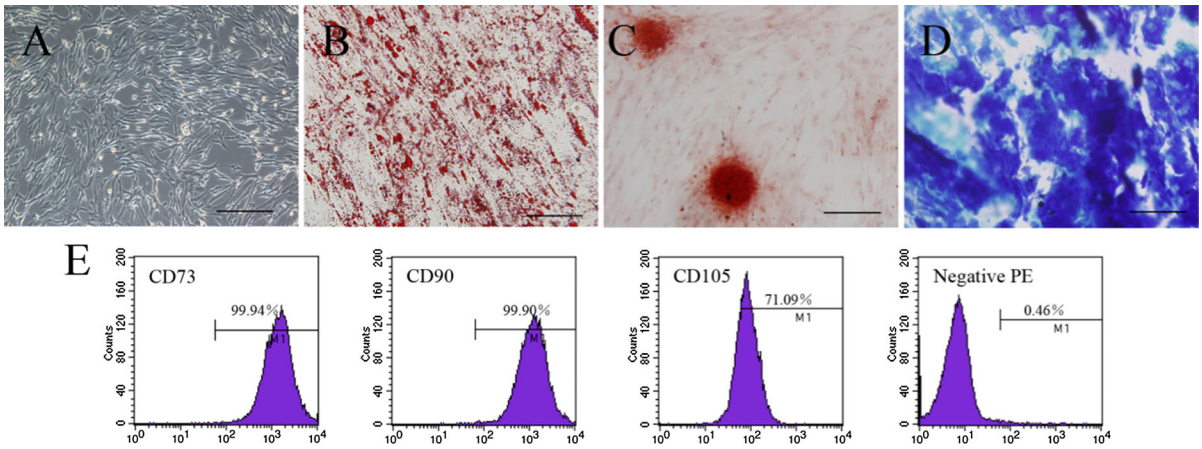

Fig. 2 Biological characterization of human umbilical cord-derived mesenchymal stem cells (hUCMSCs). **a** Image of passage 3 (P3) hUCMSCs under a phase-contrast microscope. **b–d** The pluripotent differentiation potential of hUCMSCs for differentiation into adipogenic (**b**, oil red O staining), osteogenic (**c**, alizarin red staining), and chondrogenic lineages (**d**, alcian blue staining) when cultured in different types of lineage-specific medium. Scale bars in **a–d**: 100 μm. **e** Positive expression of CD73, CD90, and CD105 and negative expression of PE, including CD45, CD34, CD11b, CD19, and HLA-DR surface molecules, as indicated by flow cytometry

Preparation of hUCMSC-derived ECM

After the addition of a certain amount of ascorbic acid to the medium for 7 days of culture, phase-contrast microscopy and SEM showed that hUCMSCs were embedded in ECM and secreted an abundance of ECM to form a cell sheet before cell removal (Fig. 3a1, b1, b3). The ECM had an intricate and fibrillar network ultrastructure that consisted of a mass of filaments after cell removal (Fig. 3a2, b2, b4). To examine the effects of decellularization on the unique composition of hUCMSC-derived ECM, immunofluorescence staining analysis was used to compare changes in collagen I, collagen II, laminin, fibronectin, decorin,

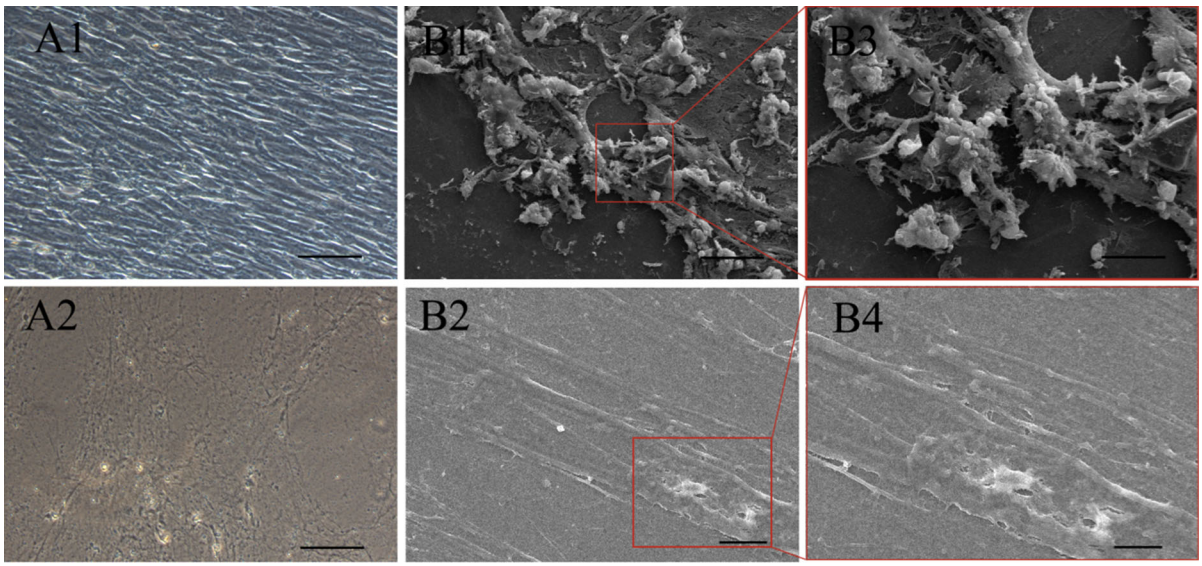

Fig. 3 Morphological observation of hUCMSC-derived extracellular matrix (ECM). **a1**, **a2**: phase-contrast images of hUCMSC-derived ECM before and after decellularization. **b1**, **b3** and **b2**, **b4**: scanning electron microscopy of hUCMSC-derived ECM before and after decellularization. The red rectangles indicate areas shown at higher magnification. Scale bars: 100 μm (**a1**, **a2**, **b1**); 10 μm (**b2**); 50 μm (**b3**); 1 μm (**b4**)

perlecan, and biglecan before and after decellularization, and Hoechst 33258 staining demonstrated hardly any residual cell nuclei after decellularization, as visualized by fluorescence microscopy (Fig. 4). We found that these proteins were randomly distributed, and cell residues were effectively removed with minimal disruption of the ECM components that help maintain ECM ultrastructure. Additionally, these proteins play important roles in cartilage tissue repair and regeneration. They provide not only attachment sites and structural support for cells but also an abundance of intrinsic and natural biological information for signaling for cell growth and behaviors, including adhesion, proliferation, and differentiation, as well as regulation of gene expression.

The hUCMSC-derived ECM microenvironment enhanced the morphology and proliferation potential of chondrocytes

To identify the effects of hUCMSC-derived ECM on the morphology and proliferation of chondrocytes, P0–P6 (P6 not shown) chondrocytes were respectively seeded on two different substrates, plastic culture plates (2D plastic) and culture plates coated with hUCMSC-derived ECM (3D ECM). 2D plastic was the control group (Fig. 5a). Under a phase-contrast

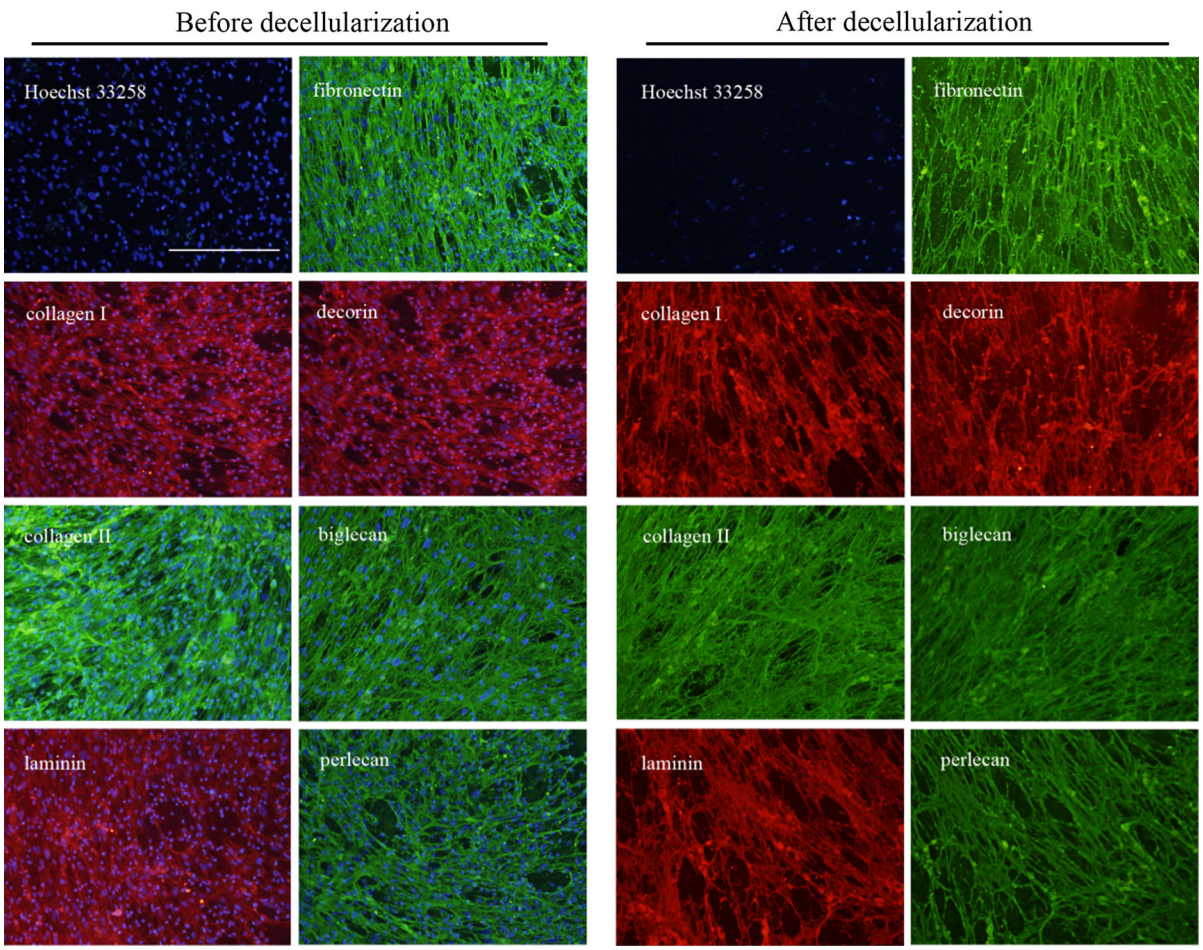

Fig. 4 Characteristics of hUCMSC-derived ECM. Immunofluorescence images indicate the localization of collagen I and II, laminin, fibronectin, decorin, biglycan, and perlecan in the ECM produced by hUCMSCs before and after decellularization. DAPI staining (blue) was used to detect the distribution of cells, and matrix proteins were visualized by confocal fluorescence images (collagen I, laminin, and decorin are stained red; collagen II, fibronectin, biglycan, and perlecan are stained green). Scale bar: 100 μm

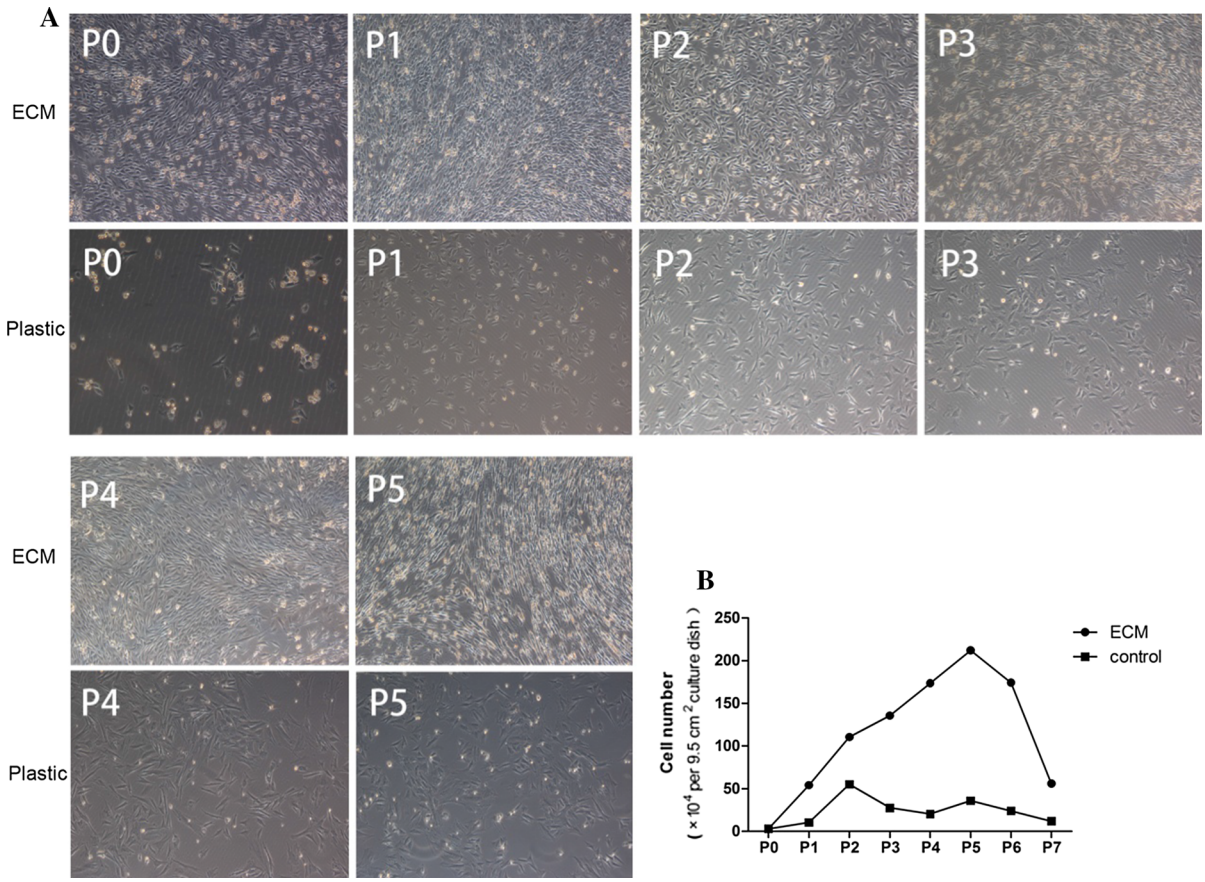

Fig. 5 Effects of hUCMSC–derived ECM on the morphology and proliferation capacity of chondrocytes. **a** P0–P5 chondrocytes cultured on either 2D plastic or 3D ECM substrate plates. Phase-contrast microscopy was used to assess chondrocyte morphological properties. **b** Cell proliferation capacity of chondrocytes grown on plastic versus ECM plates at each passage. Results are expressed as mean ± SD (n = 5)

microscope, we observed that chondrocytes cultured on ECM exhibited a fibroblast-like shape with a smaller size according to the direction of ECM compared with the original morphology, whereas chondrocytes were lenient, flattened, and more bifurcate when cultured on plastic plates, especially after P3. The number of expanded chondrocytes continued to decrease in the plastic plate group after P2; in contrast, the expanded cell number increased from P1 to P5 in the ECM plate group, which had two–ninefold more cells than that in the plastic plate group (Fig. 5b).

Cell cycle assays were used to compare the cell proliferation potential of chondrocytes expanded on the two different substrates by flow cytometry. The proportions of chondrocytes in the G1 and G2/S phase were 55.76 ± 0.70% and 44.24 ± 0.70%, respectively, in the ECM plate group and 71.68 ± 0.69% and 18.32 ± 0.69%, respectively, in the plastic plate group. It was obvious that chondrocytes expanded on ECM plates had a significantly stronger proliferative potential than those expanded on plastic plates (Fig. 6a–c). EdU (red)/Hoechst (blue) immunostaining showed the same results as those of the cell cycle assay, further confirming that hUCMSC-derived ECM was superior in promoting chondrocyte proliferation (Fig. 6d–f).

Differentiation potential of chondrocytes expanded on hUCMSC-derived ECM microenvironment

To evaluate the density and distribution of chondrocyte-secreted specific matrix, histology and immunohistochemical stainings were performed on days 7 and

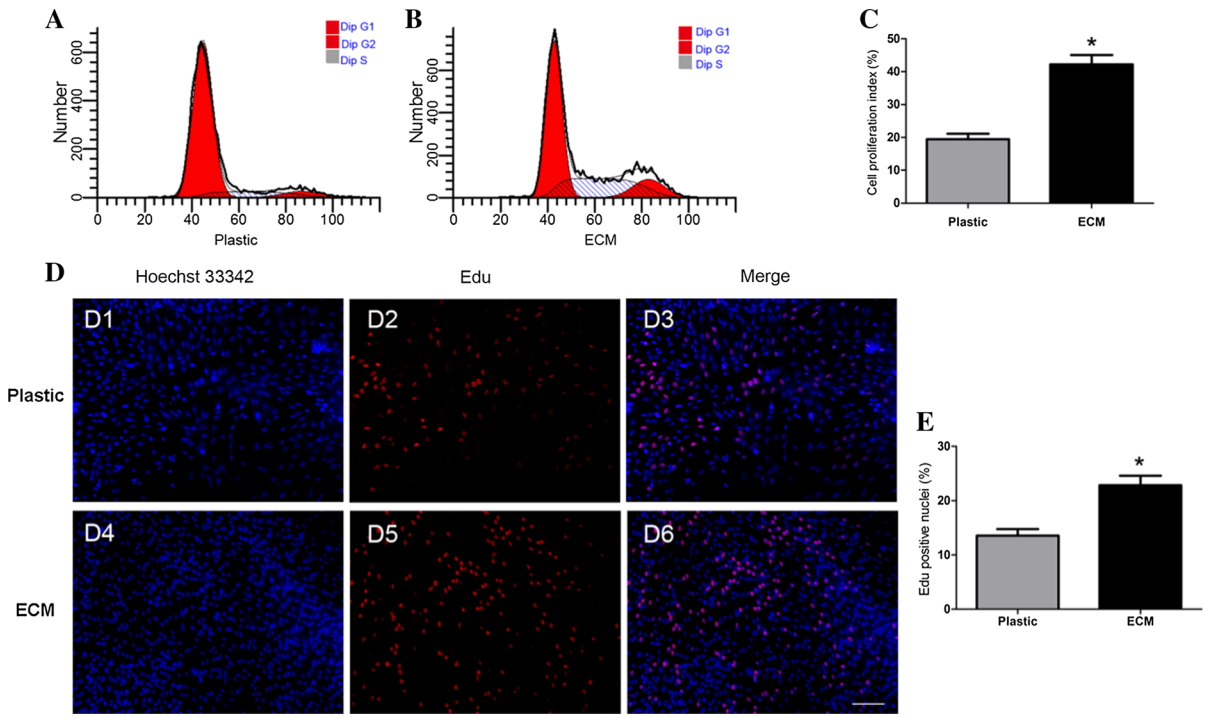

Fig. 6 Effect of hUCMSC–derived ECM on the proliferation capacity of chondrocytes. **a**, **b**: Cell cycle analysis by flow cytometry using propidium iodide (PI) staining. **c**: Comparison of the proliferative index of chondrocytes cultured on ECM versus plastic plates. **d**: Hoechst 33342 (blue) and 5-ethynyl-2′-deoxyuridine (EdU) (red) immunofluorescence staining of chondrocytes grown on plastic and ECM plates. Scale bar: 50 μm. **e**: Comparison of the EdU-positive nuclei of chondrocytes in the plastic control versus ECM plate groups. $*p < 0.05$, $**p < 0.01$ versus chondrocytes cultured on plastic in the two histograms. Results are expressed as mean ± SD (n = 5)

14 (Fig. 7). We found much stronger toluidine blue and collagen II immunohistochemical staining in the ECM plate group than in the plastic plate group 7 and 14 days after induction, but the staining of collagen I was weaker. The results indicated that sulfated GAGs and collagen II were distributed more densely around chondrocytes in the ECM plate group.

To confirm the histological results, biochemical analysis was performed to quantify DNA and GAGs in the chondrocytes cultured on ECM or plastic plates on days 3, 7, and 14 (Fig. 8). By measuring DNA content, we found that, chondrocytes exhibited time-dependent increases in cell number of approximately 37% and 98% after 7 days and approximately 235% and 256% after 14 days of culture on the plastic and ECM substrates, respectively, compared with the numbers of cells on day 3 (Fig. 8a). Meanwhile, the GAG content increased by approximately 70% and 137% after 7 days and approximately 308% and 321% after 14 days of culture on the plastic and ECM substrates, respectively, compared with the GAG level secreted by chondrocytes on day 3 (Fig. 8b). We found that both the DNA and GAG contents increased over time in cells incubated on both substrates ($p \leq 0.01$; day 7 vs. day 3; day 14 vs. day 7). To further evaluate GAG secretion by chondrocytes, we calculated the ratio of GAG to DNA content, which was used as a chondrogenic index. The chondrocytes cultured on ECM had a higher chondrogenic index than did those cultured on plastic for 3, 7, and 14 days after induction, as demonstrated by the GAG content analysis. The chondrogenic index increased over time from days 3 to 7 ($p \leq 0.05$; Fig. 8c). Therefore, hUCMSC-derived ECM enhanced the GAG synthesis and differentiation potential of chondrocytes.

To evaluate the effects of hUCMSC-derived ECM on the chondrocytes at the genetic level, RT-PCR (Fig. 9a, b) was used to quantify the mRNA levels of Collagen I and II, Aggrecan, and Sox9 (chondrogenic marker genes), and Collagen X (hypertrophic marker gene) on days 7 and 14. The gene expression results showed that the levels of Collagen II, SOX9, and

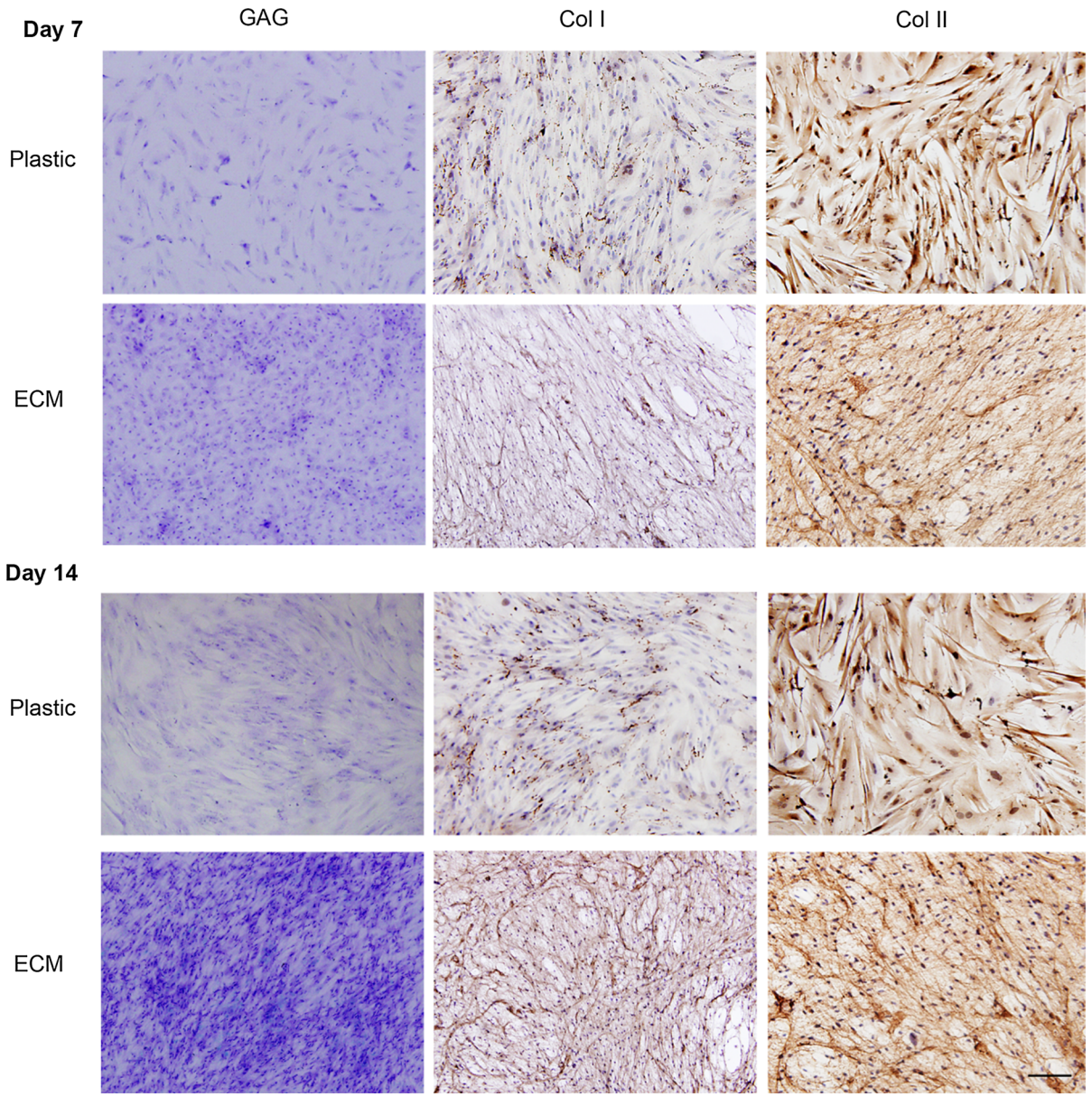

Fig. 7 Effect of hUCMSC–derived ECM on the differentiation potential of expanded chondrocytes at the matrix protein level. Toluidine blue staining was performed to detect sulfated glycosaminoglycans (GAGs) and immunostaining to detect collagens I and II. Scale bars: 100 μm

Aggrecan increased over 14 days in both the ECM and plastic plate groups, but there was no significant difference in the level of Collagen I gene expression. Collagen II, SOX9, and Aggrecan displayed higher expression levels in chondrocytes cultured on ECM compared with plastic at 7 and 14 days. In contrast, the expression of Collagen X was lower in the ECM than the plastic plate group.

Discussion

Cartilage damage has always been a common orthopedic disease, as the lack of blood vessels and nerves in cartilage severely limits self-repair capacity; thus, the repair of articular cartilage damage is an immense clinical challenge in the field of orthopedics (Redman et al. 2005). The ACT technique is currently the most

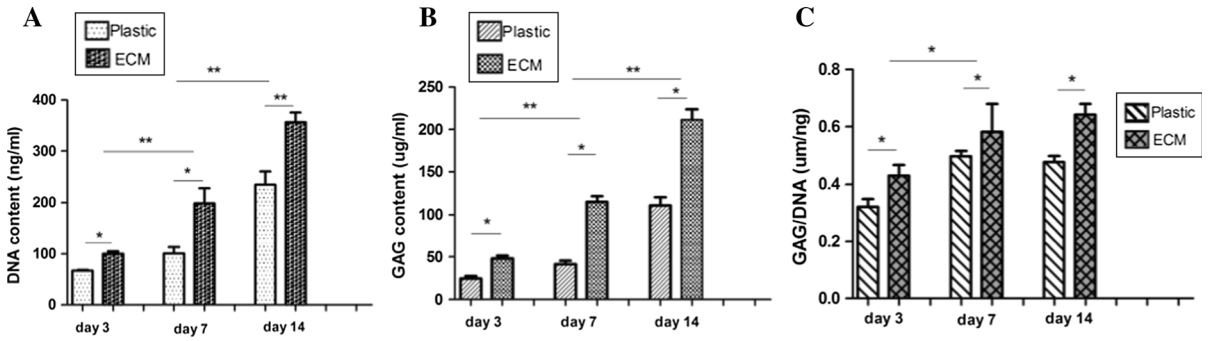

Fig. 8 Differentiation potential of expanded chondrocytes cultured on two different substrates. Biochemical analyses were used to detect DNA content, GAG content, and the GAG to DNA content ratio. $*p < 0.05$; $**p < 0.01$. Results are expressed as mean ± SD (n = 5)

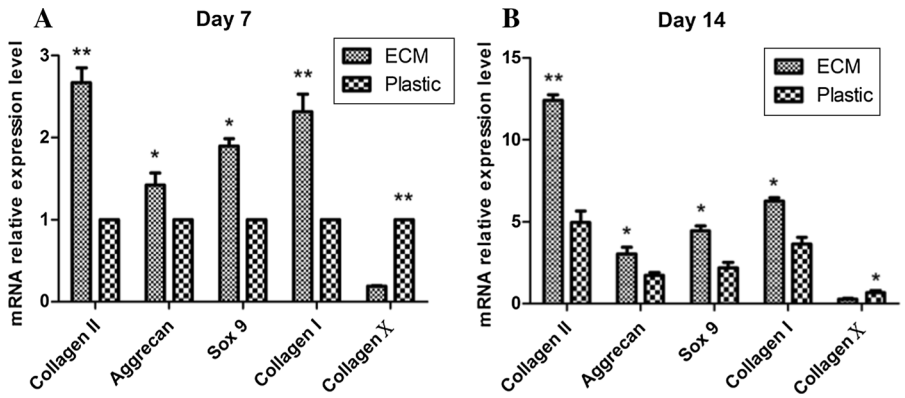

Fig. 9 Differentiation potential at the mRNA level of expanded chondrocytes cultured on two different substrates. RT-PCR analyses were used to measure the expression levels of collagen II, aggrecan, Sox9, collagen I, and collagen X in expanded chondrocytes cultured on ECM and plastic plates on day 7 (**a**) and day 14 (**b**). $*p < 0.05$; $**p < 0.01$. Results are expressed as mean ± SD (n = 5)

common and promising strategy for cartilage repair and shows excellent therapeutic effects (Beris et al. 2012). However, this technique still has several disadvantages, such as the limited number of autologous cells, donor site morbidity, and loss of chondrocyte characteristics along with monolayer cell expansion. Thus, methods to improve the quantity and quality of seed cells have become key factors in the development of cartilage tissue engineering and regeneration.

In this study, we developed a method for preparing a novel in vitro cell culture system using hUCMSC-derived ECM, which more closely mimics the cartilaginous niche and supports the proliferation and differentiation of chondrocytes. The effects of cell-derived ECM on cells are due to its biophysical and biochemical properties as a biophysical template with bulk stiffness, porosity, and surface topography that provides both structural and biomechanical support for the adhesion, migration, differentiation, and growth of cells, which in turn can sense the external forces and stiffness of the surrounding ECM and adjust themselves to adapt to the local microenvironment. The cell-derived ECM also acts as a biochemical reservoir of cell-generated bioactive signaling molecules, such as TGF-β, BMP-2, and insulin-like growth factor-1, and can anchor cell surface receptors and regulate cell behavior (DuFort et al. 2011; Kim et al. 2015).

At present, cell-derived ECM substrates should by prepared by removing cellular components as much as possible, while minimizing the loss of major matrix components and ultrastructure, to better retain biocompatibility and biomechanical strength (Gilbert et al. 2006). However, there are currently no unified

standards for decellularization. Normally, according to the cell type, cell density, ECM thickness, or water content, we select a specific decellularization method (Crapo et al. 2011). Mild detergents (Triton X-100) and alkaline reagents (ammonium hydroxide) are used to lyse cells, and biological agents, particularly nucleases (DNase and RNase), are sometimes applied to remove residual DNA or RNA. Hence, the preparation of hUCMSC-derived ECM usually involves a combination of chemical and biological digestions. The process of decellularization is key for eliminating the components and antigenicity of cells, as well as reducing inflammatory and immune responses. A recent study suggested that adding a certain amount of ascorbic acid to the medium prior to decellularization facilitates ECM deposition and cell sheet formation. Guo et al. found 50 mg/mL vitamin C in medium to be the optimal concentration (Guo et al. 2015).

To observe the microstructure of hUCMSC-derived ECM, we used light microscopy and SEM. The results showed that the microstructure of the hUCMSC-derived ECM existed both before and after decellularization, and the ECM exhibited a 3D structure with many lacunae that was conducive for cell adhesion, growth, and cell–matrix interactions. The topology of the hUCMSC-derived ECM suggests an important basis for hybrid scaffold applications. To characterize the hUCMSC-derived ECM, immunohistochemical staining was used to identify different molecules. These primary components of ECM constitute an intricate network that can supply a suitable niche for cartilage regeneration. The immunohistochemical staining results indicated that hUCMSC-derived ECM consists mainly of fibrillar components including collagens I and II, small leucine-rich PGs including decorin, perlecan, and biglecan, and adhesion glycoproteins including fibronectin and laminin. Collagens and PGs make up the basic frame of the fiber mesh complex on the cell surface and endow a certain strength and elasticity to the complex. Additionally, the fiber mesh complex can anchor surface receptors on the cell with fibronectin and laminin, and integrin, one of the crucial cell surface transmembrane receptors, may connect protein components to the intracellular cytoskeleton and reinforce interactions between the ECM and cells (Legate et al. 2009). Integrins have been shown to regulate cell proliferation, adhesion, and differentiation by activating the phosphoinositide 3-kinase and focal adhesion kinase signaling pathways (Buitenhuis 2011; Legate et al. 2009). Some antibodies or small-molecule drugs may hinder the function of integrins in clinical practice. In summary, the primary components of hUCMSC-derived ECM, including collagens, fibronectin, laminin, decorin, perlecan, and biglecan, form a fiber mesh complex with specialized biophysical, biomechanical, and biochemical properties that may directly or indirectly influence cell phenotype, behavior, and fate.

Our results showed that the hUCMSC-derived ECM was better than plastic at promoting the proliferation and differentiation of chondrocytes, and that the chondrocytes exhibited the morphological features of young cells (fibroblast-like shape and smaller size). This suggests that ECM is more suitable for chondrocyte growth than is plastic. The potential mechanism by which ECM enhances the chondrocyte proliferation and differentiation capacity may be facilitation of the interactions between ECM and cells via different signaling transduction pathways. However, it is still unclear which molecular components of hUCMSC-derived ECM play crucial roles in this potential mechanism; thus, further research is required. Meanwhile, the RT-PCR data indicated higher expression of chondrogenic marker genes (Collagen II, Aggrecan, and Sox9) and lower expression of the hypertrophic marker gene, Collagen X, in the ECM than in the plastic plate group. These genes not only contribute to the proliferation capacity of chondrocytes but also enhance differentiation capacity. Furthermore, cell-derived ECM also promotes Schwann cell proliferation and neurite growth (Xiao et al. 2016), as well as retention of stemness in MSCs (Xiong et al. 2015). These results suggest that cell-derived ECM provides an appropriate microenvironment for cell growth and will play a key role in the development of cell implantation techniques.

Conclusions

In this study, we used a protocol to reconstruct a novel 3D cell culture system using hUCMSC-derived ECM, which potentially provides an appropriate stem cell niche for chondrocyte growth. In vitro culture experiments showed that hUCMSC-derived ECM enhanced the proliferation and differentiation capacity of chondrocytes. This suggests that hUCMSC-derived ECM will improve chondrocyte quantity and quality for

cartilage tissue engineering and regeneration technology in future clinical applications. Currently, many cell-derived ECM biomaterials have become important candidate materials as ECM scaffolds or ECM hybrid scaffolds for tissue engineering, because they have superior biophysical, biomechanical, and biochemical properties that play key roles in cell proliferation, differentiation, migration, and retention of stemness in biological processes. Future tissue engineering studies should explore the potential mechanisms of ECM involvement in cartilage regeneration and identify molecules that play major roles in the underlying mechanisms.

Acknowledgements This work was supported by the National Basic Research Program of China (973, 2014CB542201), and the People's Liberation Army 12th 5-year plan period (BWS11J025).

Compliance with ethical standards

Conflict of interest No competing financial interests exist.

Ethical statement This research was approved by our institutional review board.

References

Antebi B, Zhang Z, Wang Y, Lu Z, Chen XD, Ling J (2015) Stromal-cell-derived extracellular matrix promotes the proliferation and retains the osteogenic differentiation capacity of mesenchymal stem cells on three-dimensional scaffolds. Tissue Eng C Methods 21:171–181

Arrich J, Piribauer F, Mad P, Schmid D, Klaushofer K, Mullner M (2005) Intra-articular hyaluronic acid for the treatment of osteoarthritis of the knee: systematic review and meta-analysis. CMAJ 172:1039–1043

Benya PD, Shaffer JD (1982) Dedifferentiated chondrocytes reexpress the differentiated collagen phenotype when cultured in agarose gels. Cell 30:215–224

Beris AE, Lykissas MG, Kostas-Agnantis I, Manoudis GN (2012) Treatment of full-thickness chondral defects of the knee with autologous chondrocyte implantation: a functional evaluation with long-term follow-up. Am J Sports Med 40:562–567

Buckwalter JA, Mankin HJ (1998) Articular cartilage: degeneration and osteoarthritis, repair, regeneration, and transplantation. Instr Course Lect 47:487–504

Buitenhuis M (2011) The role of PI3K/protein kinase B (PKB/c-akt) in migration and homing of hematopoietic stem and progenitor cells. Curr Opin Hematol 18:226–230

Chen XD, Dusevich V, Feng JQ, Manolagas SC, Jilka RL (2007) Extracellular matrix made by bone marrow cells facilitates expansion of marrow-derived mesenchymal progenitor cells and prevents their differentiation into osteoblasts. J Bone Miner Res 22:1943–1956

Crapo PM, Gilbert TW, Badylak SF (2011) An overview of tissue and whole organ decellularization processes. Biomaterials 32:3233–3243

Dominici M, Le Blanc K, Mueller I, Slaper-Cortenbach I, Marini F, Krause D, Deans R, Keating A, Prockop D, Horwitz E (2006) Minimal criteria for defining multipotent mesenchymal stromal cells. The International Society for Cellular Therapy position statement. Cytotherapy 8:315–317

Du P, Subbiah R, Park JH, Park K (2014) Vascular morphogenesis of human umbilical vein endothelial cells on cell-derived macromolecular matrix microenvironment. Tissue Eng A 20:2365–2377

DuFort CC, Paszek MJ, Weaver VM (2011) Balancing forces: architectural control of mechanotransduction. Nat Rev Mol Cell Biol 12:308–319

Gelber AC, Hochberg MC, Mead LA, Wang NY, Wigley FM, Klag MJ (2000) Joint injury in young adults and risk for subsequent knee and hip osteoarthritis. Ann Intern Med 133:321–328

Gilbert TW, Sellaro TL, Badylak SF (2006) Decellularization of tissues and organs. Biomaterials 27:3675–3683

Gu Y, Zhu J, Xue C, Li Z, Ding F, Yang Y, Gu X (2014) Chitosan/silk fibroin-based, Schwann cell-derived extracellular matrix-modified scaffolds for bridging rat sciatic nerve gaps. Biomaterials 35:2253–2263

Guo P, Zeng JJ, Zhou N (2015) A novel experimental study on the fabrication and biological characteristics of canine bone marrow mesenchymal stem cells sheet using vitamin C. Scanning 37:42–48

He F, Chen X, Pei M (2009) Reconstruction of an in vitro tissue-specific microenvironment to rejuvenate synovium-derived stem cells for cartilage tissue engineering. Tissue Eng A 15:3809–3821

Hunziker EB (1999) Articular cartilage repair: are the intrinsic biological constraints undermining this process insuperable? Osteoarthritis Cartilage 7:15–28

Hurd SA, Bhatti NM, Walker AM, Kasukonis BM, Wolchok JC (2015) Development of a biological scaffold engineered using the extracellular matrix secreted by skeletal muscle cells. Biomaterials 49:9–17

Hynes RO (2009) The extracellular matrix: not just pretty fibrils. Science 326:1216–1219

Jian R, Yixu Y, Sheyu L, Jianhong S, Yaohua Y, Xing S, Qingfeng H, Xiaojian L, Lei Z, Yan Z, Fangling X, Huasong G, Yilu G (2015) Repair of spinal cord injury by chitosan scaffold with glioma ECM and SB216763 implantation in adult rats. J Biomed Mater Res A 103:3259–3272

Kim IG, Hwang MP, Du P, Ko J, Ha CW, Do SH, Park K (2015) Bioactive cell-derived matrices combined with polymer mesh scaffold for osteogenesis and bone healing. Biomaterials 50:75–86

Lai Y, Sun Y, Skinner CM, Son EL, Lu Z, Tuan RS, Jilka RL, Ling J, Chen XD (2010) Reconstitution of marrow-derived extracellular matrix ex vivo: a robust culture system for expanding large-scale highly functional human mesenchymal stem cells. Stem Cells Dev 19:1095–1107

Lane SW, Williams DA, Watt FM (2014) Modulating the stem cell niche for tissue regeneration. Nat Biotechnol 32:795–803

Legate KR, Wickstrom SA, Fassler R (2009) Genetic and cell biological analysis of integrin outside-in signaling. Genes Dev 23:397–418

Li J, Pei M (2012) Cell senescence: a challenge in cartilage engineering and regeneration. Tissue Eng B Rev 18:270–287

Li J, Hansen KC, Zhang Y, Dong C, Dinu CZ, Dzieciatkowska M, Pei M (2014) Rejuvenation of chondrogenic potential in a young stem cell microenvironment. Biomaterials 35:642–653

Liao J, Guo X, Grande-Allen KJ, Kasper FK, Mikos AG (2010) Bioactive polymer/extracellular matrix scaffolds fabricated with a flow perfusion bioreactor for cartilage tissue engineering. Biomaterials 31:8911–8920

Ng CP, Sharif AR, Heath DE, Chow JW, Zhang CB, Chan-Park MB, Hammond PT, Chan JK, Griffith LG (2014) Enhanced ex vivo expansion of adult mesenchymal stem cells by fetal mesenchymal stem cell ECM. Biomaterials 35:4046–4057

Ozbek S, Balasubramanian PG, Chiquet-Ehrismann R, Tucker RP, Adams JC (2010) The evolution of extracellular matrix. Mol Biol Cell 21:4300–4305

Pei M, He F (2012) Extracellular matrix deposited by synovium-derived stem cells delays replicative senescent chondrocyte dedifferentiation and enhances redifferentiation. J Cell Physiol 227:2163–2174

Pei M, He F, Li J, Tidwell JE, Jones AC, McDonough EB (2013) Repair of large animal partial-thickness cartilage defects through intraarticular injection of matrix-rejuvenated synovium-derived stem cells. Tissue Eng A 19:1144–1154

Peng J, Wang Y, Zhang L, Zhao B, Zhao Z, Chen J, Guo Q, Liu S, Sui X, Xu W, Lu S (2011) Human umbilical cord Wharton's jelly-derived mesenchymal stem cells differentiate into a Schwann-cell phenotype and promote neurite outgrowth in vitro. Brain Res Bull 84:235–243

Pham QP, Kasper FK, Scott Baggett L, Raphael RM, Jansen JA, Mikos AG (2008) The influence of an in vitro generated bone-like extracellular matrix on osteoblastic gene expression of marrow stromal cells. Biomaterials 29:2729–2739

Redman SN, Oldfield SF, Archer CW (2005) Current strategies for articular cartilage repair. Eur Cells Mater 9:23–32 **(discussion 23–32)**

Schinhan M, Gruber M, Vavken P, Dorotka R, Samouh L, Chiari C, Gruebl-Barabas R, Nehrer S (2012) Critical-size defect induces unicompartmental osteoarthritis in a stable ovine knee. J Orthop Res 30:214–220

Simon TM, Jackson DW (2006) Articular cartilage: injury pathways and treatment options. Sports Med Arthrosc Rev 14:146–154

Stufkens SA, Knupp M, Horisberger M, Lampert C, Hintermann B (2010) Cartilage lesions and the development of osteoarthritis after internal fixation of ankle fractures: a prospective study. J Bone Joint Surg Am 92:279–286

von der Mark K, Gauss V, von der Mark H, Muller P (1977) Relationship between cell shape and type of collagen synthesised as chondrocytes lose their cartilage phenotype in culture. Nature 267:531–532

Watt FM, Huck WT (2013) Role of the extracellular matrix in regulating stem cell fate. Nat Rev Mol Cell Biol 14:467–473

Xiao B, Rao F, Guo ZY, Sun X, Wang YG, Liu SY, Wang AY, Guo QY, Meng HY, Zhao Q, Peng J, Wang Y, Lu SB (2016) Extracellular matrix from human umbilical cord-derived mesenchymal stem cells as a scaffold for peripheral nerve regeneration. Neural Regener Res 11:1172–1179

Xiong Y, He J, Zhang W, Zhou G, Cao Y, Liu W (2015) Retention of the stemness of mouse adipose-derived stem cells by their expansion on human bone marrow stromal cell-derived extracellular matrix. Tissue Eng A 21:1886–1894

Yuan M, Yeung CW, Li YY, Diao H, Cheung KM, Chan D, Cheah K, Chan PB (2013) Effects of nucleus pulposus cell-derived acellular matrix on the differentiation of mesenchymal stem cells. Biomaterials 34:3948–3961

Zeitouni S, Krause U, Clough BH, Halderman H, Falster A, Blalock DT, Chaput CD, Sampson HW, Gregory CA (2012) Human mesenchymal stem cell-derived matrices for enhanced osteoregeneration. Sci Transl Med 4:132–155